Laser and Particle Beams (2005), *23*, 483–502. Printed in the USA.

DOI: 10.1017/S0263034605050676

Radiation reduction of optical solitons resulting from higher order dispersion terms in the nonlinear Schrödinger equation

ROBERT BEECH AND FREDERICK OSMAN
School of Quantitative Methods & Mathematical Sciences, University of Western Sydney, Penrith South DC, Australia
(RECEIVED 2 FEBRUARY 2005; ACCEPTED 30 March 2005)

Abstract

This paper will present the nonlinearity and dispersion effects involved in propagation of optical solitons, which can be understood by using a numerical routine to solve the nonlinear Schrödinger equation (NLSE). Here, Mathematica v5© (Wolfram, 2003) is used to explore in depth several features of optical solitons formation and propagation. These numerical routines were implemented through the use of Mathematica v5© and the results give a very clear idea of this interesting and important practical phenomenon. It is hoped that this work will open up an important new approach to the cause, effect, and correction of interference from secondary radiation found in the uses of soliton waves in lasers and in optical fiber telecommunication. It is believed that these results will be of considerable use in any work or research in this field and in self-focusing properties of the soliton (Osman *et al.*, 2004*a*, 2004*b*; Hora, 1991). In a previous paper on this topic (Beech & Osman, 2004), it was shown that solitons of NLSE radiate. This paper goes on from there to show that these radiations only occur in solitons derived from cubic, or odd-numbered higher orders of NLSE, and that there are no such radiations from solitons of quadratic, or even-numbered higher order of NLSE. It is anticipated that this will stimulate research into practical means to control or eliminate such radiations.

Keywords: Higher order dispersion; Higher order of NLSE; Nonlinear Schrödinger equation (NLSE); Soliton radiations; Solitons

1. INTRODUCTION

The field of nonlinear optics has developed in recent years as nonlinear materials have become available, and widespread applications have become apparent. This is particularly true for optical solitons and other types of nonlinear pulse transmission in optical fibers and laser plasma interaction (Osman *et al.*, 2000, 2004*a*, 2004*b*; Hora, 2004). This form of light propagation can be utilized in the future for very high capacity dispersion-free communications. The purpose of this paper is to describe the use of a very powerful tool to solve the generalized nonlinear Schrödinger equation (NLSE) that has stable solutions called optical solitons (Drazin & Johnson, 1990). The solitary wave (or soliton) is a wave that consists of a single symmetrical hump that propagates at uniform velocity without changing its form. The physical origin of solitons is the Kerr effect, which relies on a nonlinear dielectric constant that can balance the group dispersion in the optical propagation medium. The resulting effect of this balance is the propagation of solitons, which has the form of a hyperbolic secant (Zakharov & Shabat, 1972).

Address correspondence and reprint requests to: F. Osman, School of Quantitative Methods & Mathematical Sciences, University of Western Sydney, Locked Bag 1797, Penrith South DC 1797, Australia. E-mail: f.osman@uws.edu.au

2. NONLINEAR SCHRÖDINGER EQUATION

The nonlinear Schrödinger equation (NLSE) used in this paper is generalized as:

$$i\frac{\partial u}{\partial \tau} + \frac{1}{2}\frac{\partial^2 u}{\partial \xi^2} + |u|^2 u = -i\gamma u + \delta_n \frac{\partial^n u}{\partial \xi^n}, \tag{1}$$

where n is the order of dissipation of the Schrödinger equation being used, and δ_n is an arbitrary constant.

Akhmediev and Ankiewicz (1997) covered the third and fourth orders adequately and Karpman (1998) and Karpman and Shagalow (1999) dealt with the solution of the fifth order. The purpose of this paper is to build upon these excellent results, explaining the three-dimensional (3D) form of these solitons and extending this to cover orders six and seven and beyond. We will be using a simplified version of the Zakharov and Shabat (1972) solution to this equation as our basis for solving it numerically using Mathematica©.

The above research has indicated the presence of radiations emanating from soliton waves. This phenomenon is the subject of this research, particularly into determining which solitons, or solitons from which parenting NLSE, are emanating radiations, and ultimately how this radiation may be controlled or eliminated completely.

Practical research into soliton emissions has indicated that these emissions are largely restricted to solitons derived from the cubic NLSE, namely a higher order equation with an odd numbered power.

3. INITIAL CONDITIONS AND PROGRAMMING FOR HIGHER ORDERS

In this problem, an analogous role is played by the particular solutions of the nonlinear Schrödinger equation [8]:

$$u(z,t) = 2\eta \,\mathrm{Sech}[2\eta(z - z_0) + 8\eta\xi t] \cdot \exp[i(-2\xi x - 4(\xi^2 - \eta^2))t + \phi]. \tag{2}$$

Where η, ξ, ϕ, t, z_0 are scaling parameters traditionally used in nonlinear Schrödinger equation [8]. This form of the solution can also be known as a soliton that has a stable formation. For the purpose of this paper, we will use the simplified solution:

$$u(t,x) = 2Sech[x]^2. \tag{3}$$

z is used here as the soliton solution in a complex variable. In the Mathematica representation, the soliton is represented as a complex function in ξ, τ space. Customary care should be taken to view these symbols within their relative context.

Using this programming method, with its wide range of available iteration models available from Mathematica; we get a 3D representation of the soliton. For each graphic representation of a soliton, we plotted its contour graph. This is most helpful because the direction of movement of soliton is much clearer. It is common for the viewer to assume that the wave moves in the direction normal to its axis, in this case the ξ axis. This is not so for a soliton which moves in the direction described by the wave ridge. The contour graph also gives a clearer picture of the radiations, which are crucial to this exercise. The third plot drawn here shows the two-dimensional (2D) cross-section of the wave at the end of the time axis, in these cases mostly $\tau = 2$. In these graphs, the wave at the end of it's time axis is shown in green. The red line represents the wave at $\tau = 0$. The fourth plot given here represents the maximum possible error at time τ. The value of this information is realized when we note that this gives an accurate indication of where the radiations/wave breaking phenomenon begins. Figure 1a shows the basic soliton wave where the coefficient of dispersion is zero; there being no dispersion term.

The excellent graphics obtained from the use of this software can be used to further enhance the understanding of the motion, as well as the physical form of the soliton wave. The untrained eye does not immediately comprehend the way in which the soliton is moving here. A lifetime of watching the movement of water waves has trained the senses to automatically assume that the wave is moving along the spatial, or ξ axis.

It is also clear from this graph that there exists a small amount of radiation being emitted from the front, or bow of the basic soliton wave. This should be carefully noted here as being distinct from other types of radiation which will come into play later as we progress to higher order terms of the NLSE. By way of an explanation of this phenomenon, let us say that any object moving through its propagating medium will, in respect of its motion, produce an effect on the stability of the medium. This type of miniscule radiation is separate and distinct from that which will appear later.

Let us now observe the contour plot as shown in Figure 1b. From the outward radiations and the pointed leading edge of the wave, it is immediately clear that it is moving along the temporal, or τ axis. Please take care to note that in Figure 1a the graph is plotted from left to right, as opposed to right to left in the other graphs. Moving on to Figure 1c, we show the 2D cross-section at the outward extremity of the time axis. The green line is the value at $\tau = 2$, the red line is the basic wave form. Finally, we show in Figure 1d, the maximum error plot for this (zero) order.

A plotted range of $0 \leq \tau \leq 2$ and $-10 \leq \xi \leq 10$ is sufficient to give a clear picture of what is happening, while showing the point where the soliton starts to break up into increasingly evident radiations. Following on from the basic wave graphs, and before we progress to the results obtained, we thought it sufficiently important that we include here a wave plot showing the effect of lengthening the axes. To this end, we show Figure 2, where the time axis is extended to $\tau = 5$ and the spatial axis to $-20 \leq \xi \leq 20$. This is deemed sufficient to illustrate the expanding wave form. We therefore have limited all our other plots to the range shown for Figure 1.

Figure 3 illustrate the effect on soliton of the zero-order term, $i\gamma u$. Here we showed the effect on soliton in Figure 1 of making $\gamma = 1$. The effect is one of damping. In this plot we can clearly see that the soliton and its radiations were very effectively damped by adding a unitary coefficient to the zero order term $-i\gamma u$ in Eq. (1).

4. RESULTS

We have found by the above method that for the dispersion orders from 3 upward in odd numbers there is a point along the evolution of the coefficient for each order of dispersion where radiation becomes visibly evident.

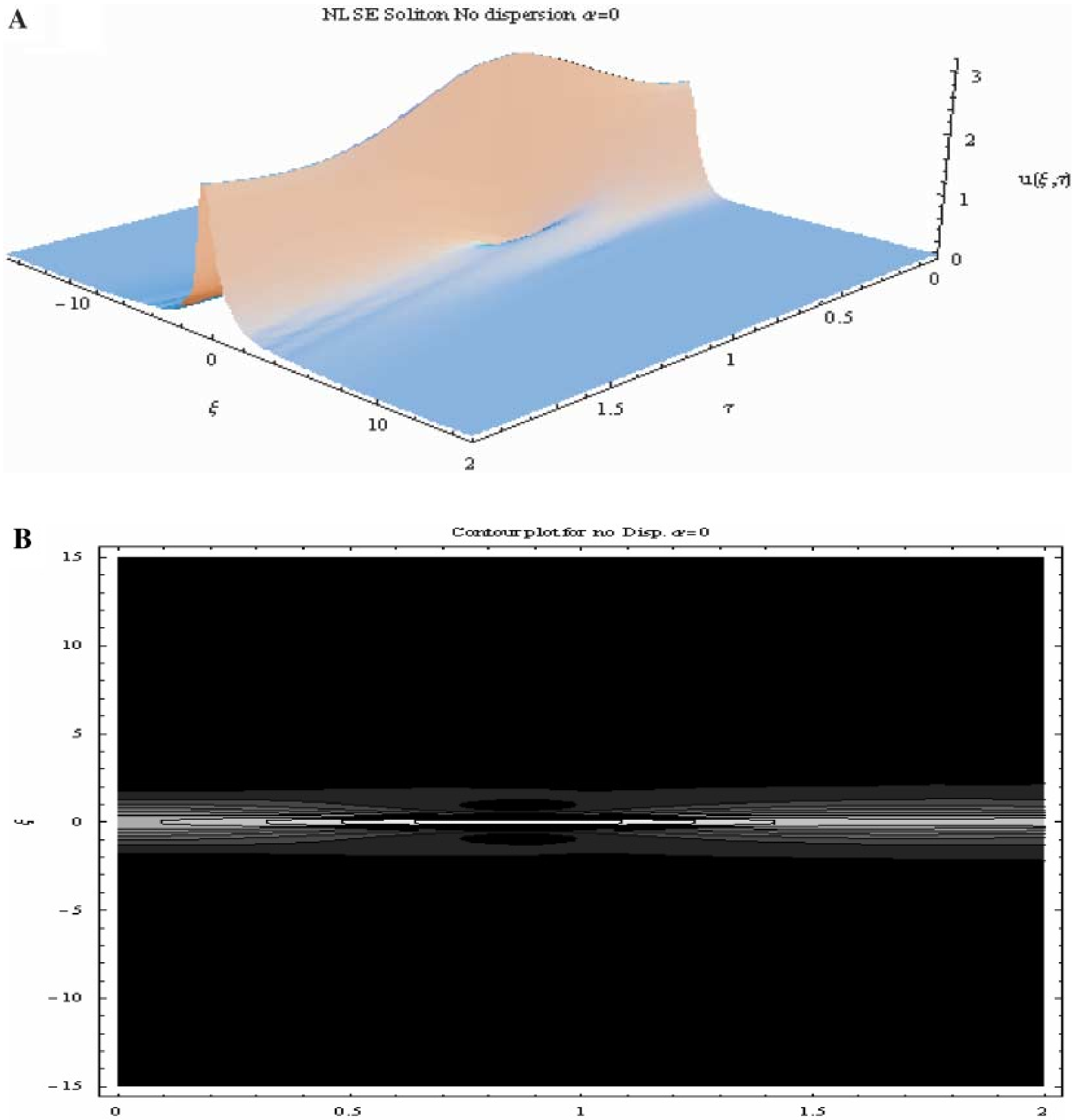

Fig. 1. (**A**) The 3D plot of the basic soliton wave. (**B**) The contour plot of the basic soliton wave.

The first wave to be shown next, in Figure 4b, is the 3D wave form for the third order soliton with dispersion coefficient 0.5. To supplement this we follow up with the Contour plot, Figure 4b, the cross-section plot, 4c and the error plot 4d. We then finish off our representation of the third order by showing the 3D soliton graph for coefficient 3.5 in Figure 5a, followed up by its contour plot in Figure 5b, its cross-section plot in Figure 5c and its error plot in Figure 5d.

For the presentation of our results we found it unnecessary to use a large number of graphs for each of the higher orders, it being sufficient to show the lowest coefficient where radiation occurs, and the last coefficient before computation overflows or the error goes beyond the point of usefulness. Consequently we show here only two sets of graphics for each of these orders.

Moving on to the fourth order, we now show the wave resulting from the fourth order term at coefficient $\alpha = 0.5$,

https://doi.org/10.1017/S0263034605050676 Published online by Cambridge University Press

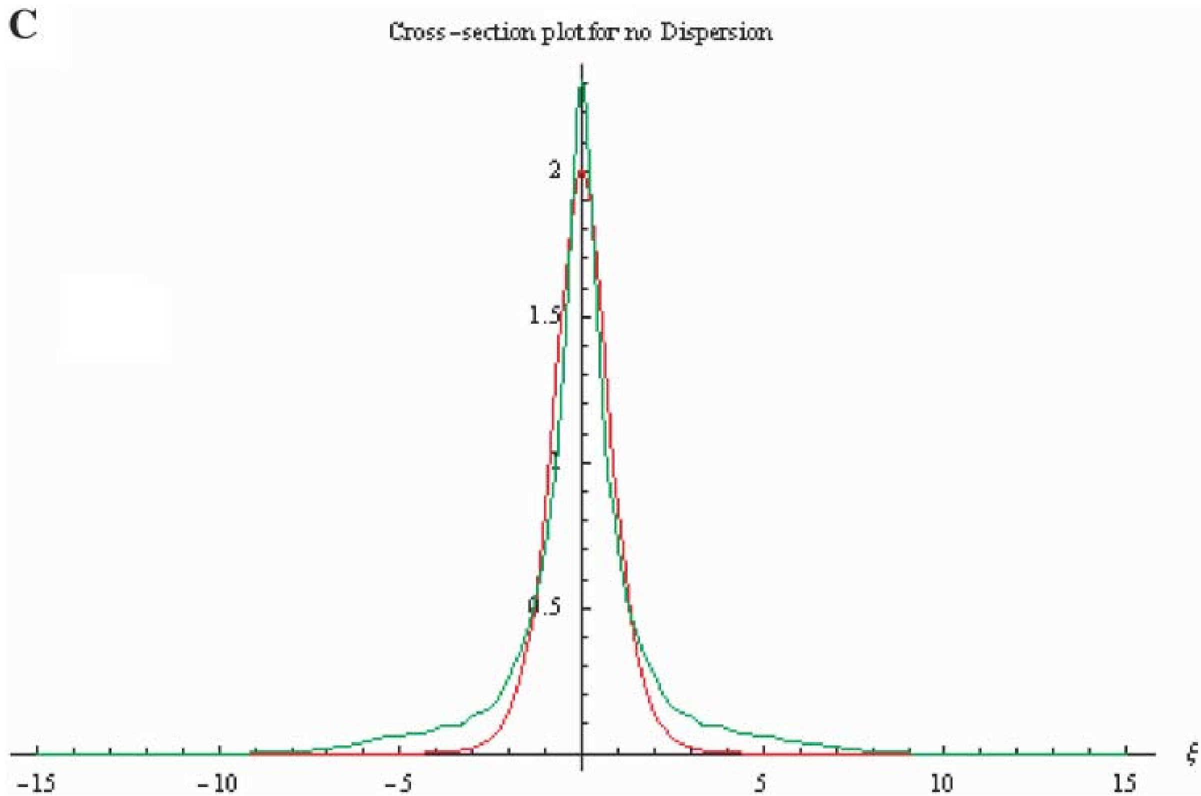

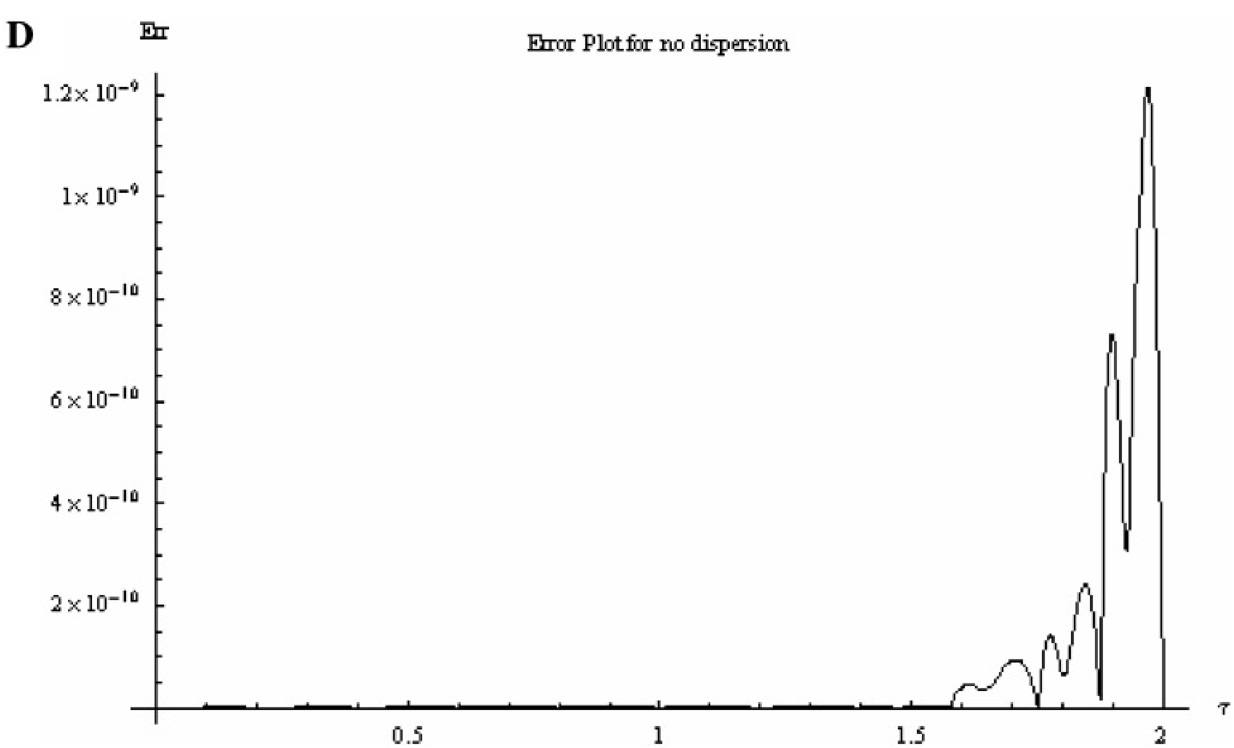

Fig. 1 (continued). (**C**) The cross-section plot for Figure 1a. The red line is the starting point, time 0, the green line is the cut-off point at time 2. (**D**) The error graph for the basic soliton wave.

https://doi.org/10.1017/S0263034605050676 Published online by Cambridge University Press

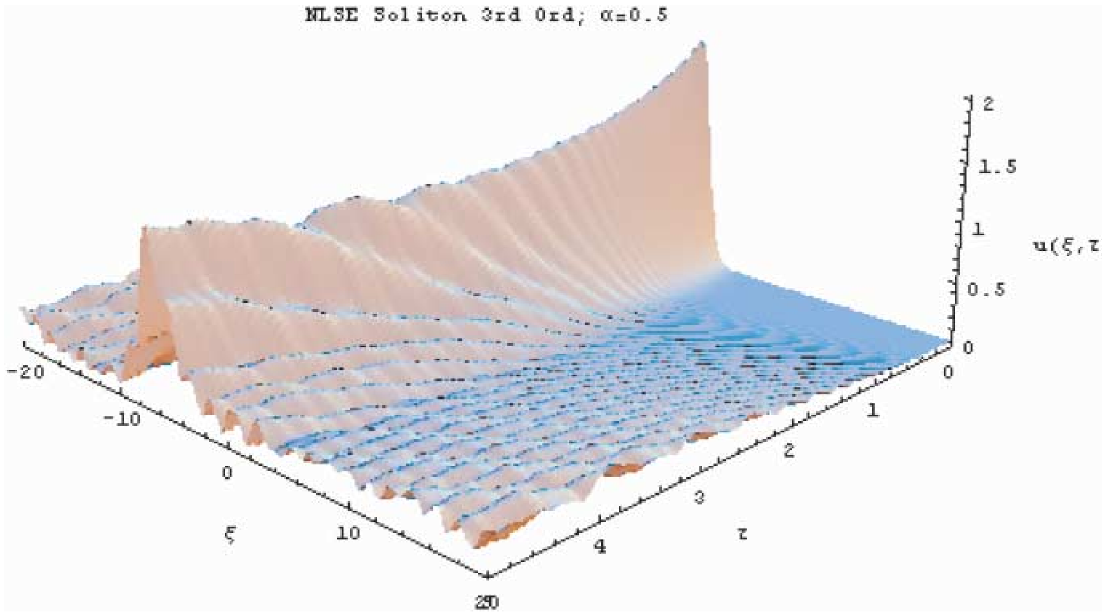

Fig. 2. This shows the same soliton as Figure 1, with extended axes. Here the viewer can see that the wave break-up, and the radiations resulting from it, increase as we progress along the time axis. It is deemed unnecessary, for further plotting, to venture beyond $\tau = 2$ in order that the perspective of this study may be maintained.

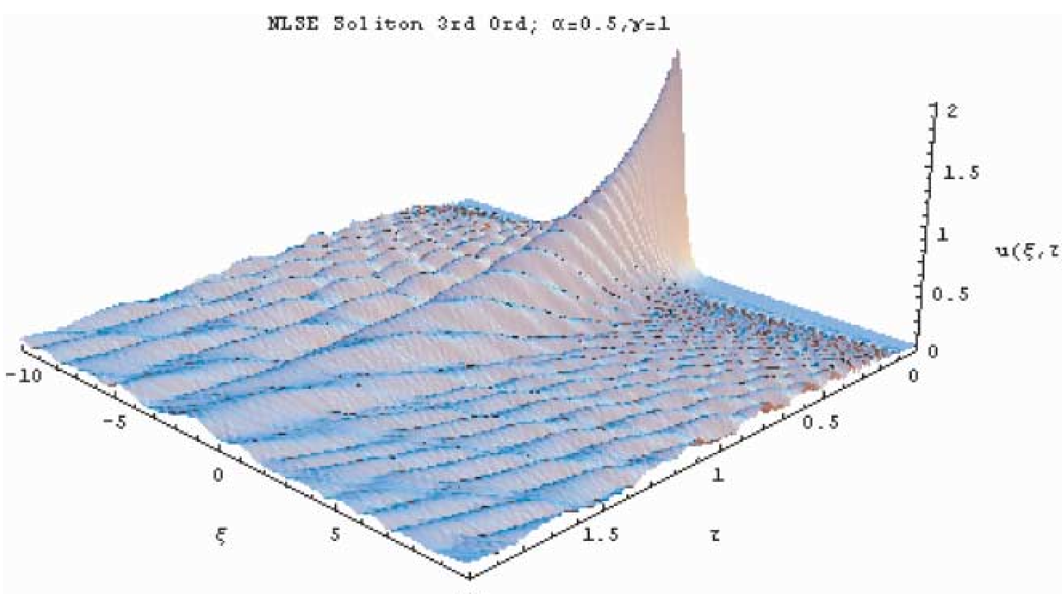

Fig. 3. The soliton in Figure 1, with the zero order term at coefficient 1. In this plot we can clearly see that the soliton and it's radiations have been very effectively damped by adding a unitary coefficient to the zero order term $-i\gamma u$ in (1).

in Figure 6a, followed by its contour plot in Figure 6b, its cross-section plot in Figure 6c and its error plot in Figure 6d. The last plot for the fourth order at coefficient 3.5 is the 3D plot in Figure 7a, followed by its contour plot in Figure 7b, its cross-section plot in Figure 7c and its error plot in Figure 7d.

Moving on to the fifth order we next show the result for lowest practical coefficient of order 5, being $\alpha = 0.01$.

Karpman (1998) and Karpman and Shagalow (1999) has defined the third and fourth order dispersion equation and this will be used throughout this work as the basis for programming the Schrödinger equation. This level of dis-

https://doi.org/10.1017/S0263034605050676 Published online by Cambridge University Press

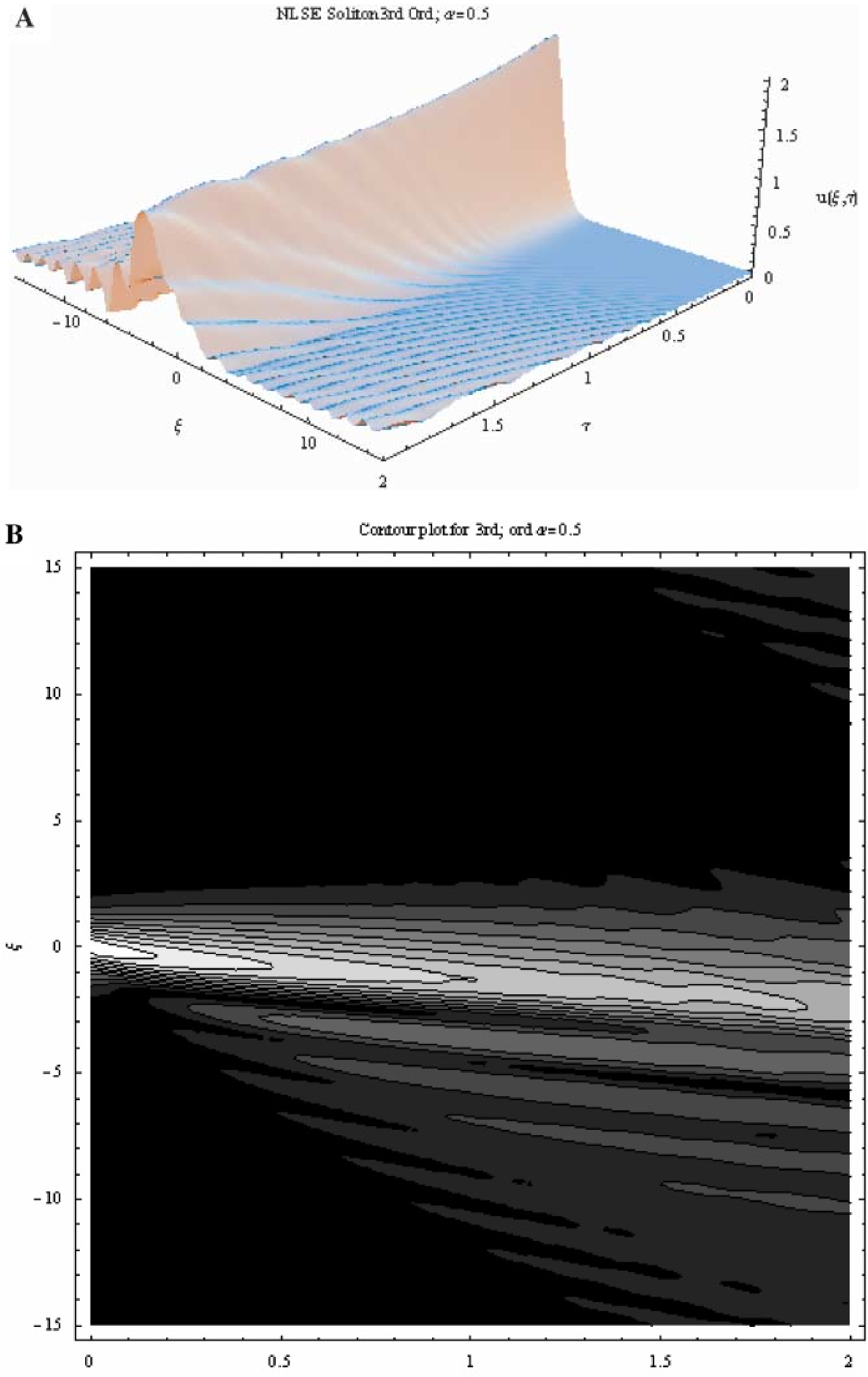

Fig. 4. (**A**) This is the wave form of the third order at dispersion coefficient 0.5. (**B**) This shows the contour plot for the wave in Figure 4a.

https://doi.org/10.1017/S0263034605050676 Published online by Cambridge University Press

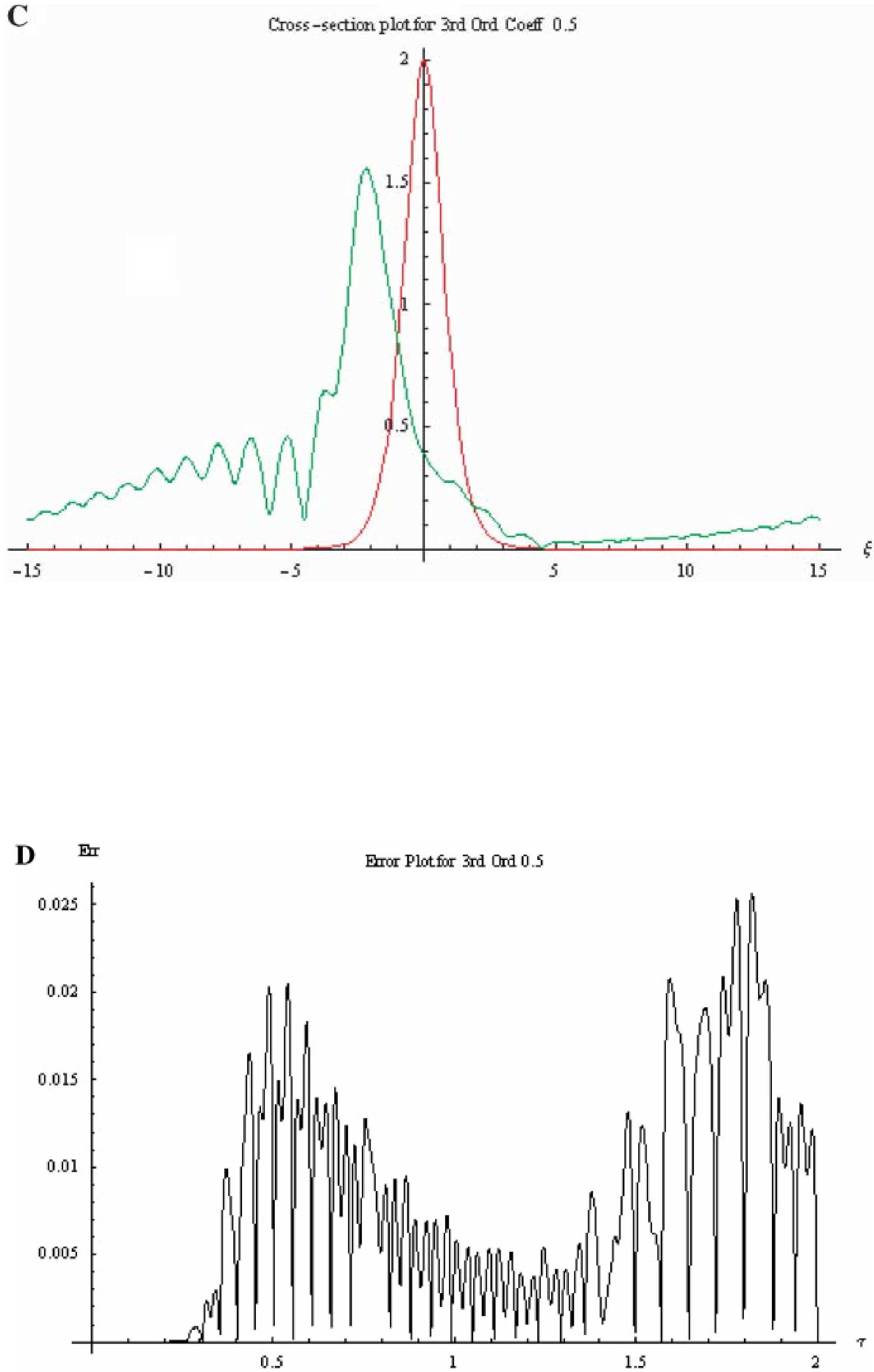

Fig. 4 (continued). (**C**) The cross-section plot for Figure 4A. (**D**) This is the error plot for the soliton in Figure 4A.

https://doi.org/10.1017/S0263034605050676 Published online by Cambridge University Press

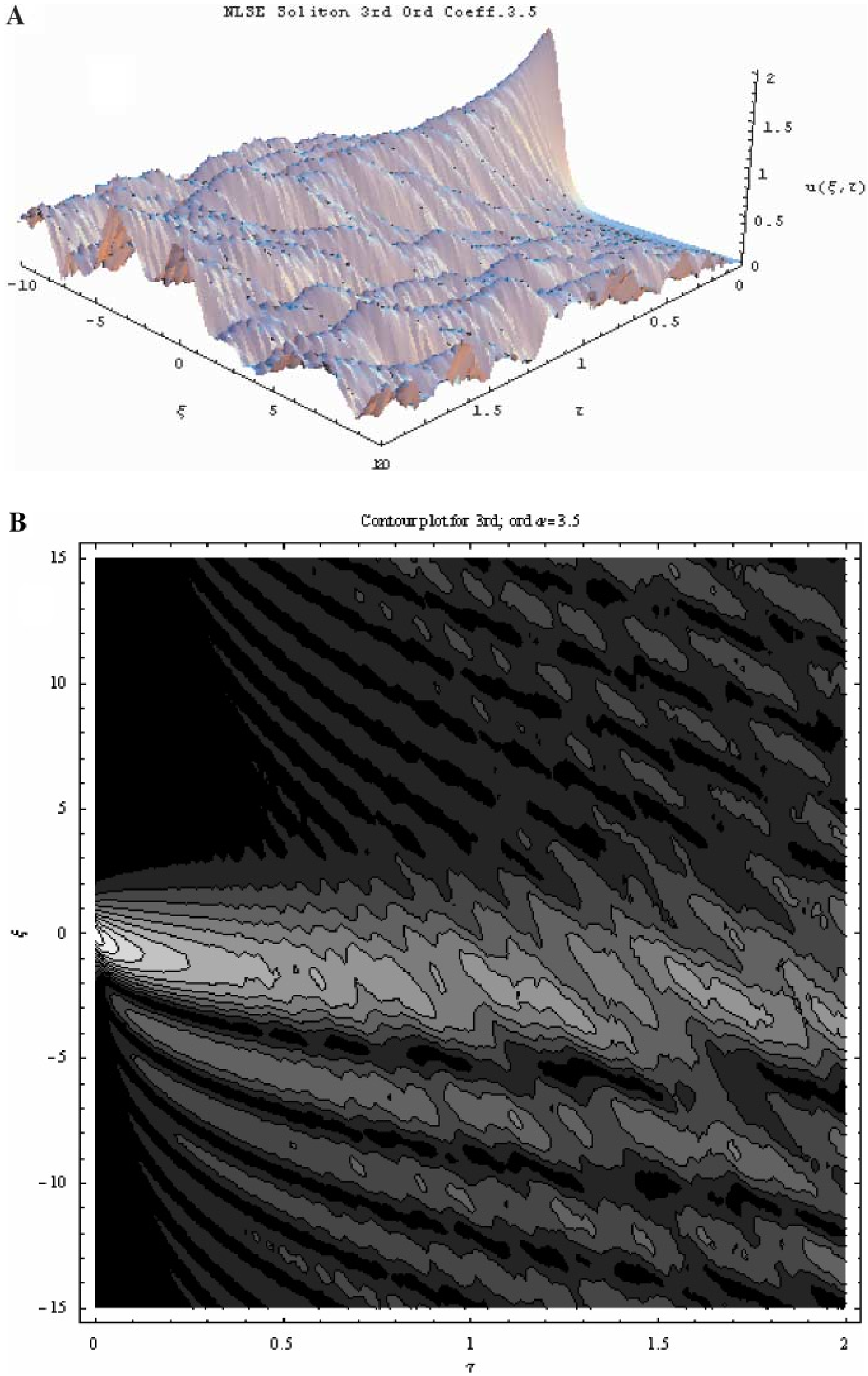

Fig. 5. (**A**) This shows the soliton at third order coefficient 3.5. (**B**) This is the contour plot for Figure 5A.

https://doi.org/10.1017/S0263034605050676 Published online by Cambridge University Press

C

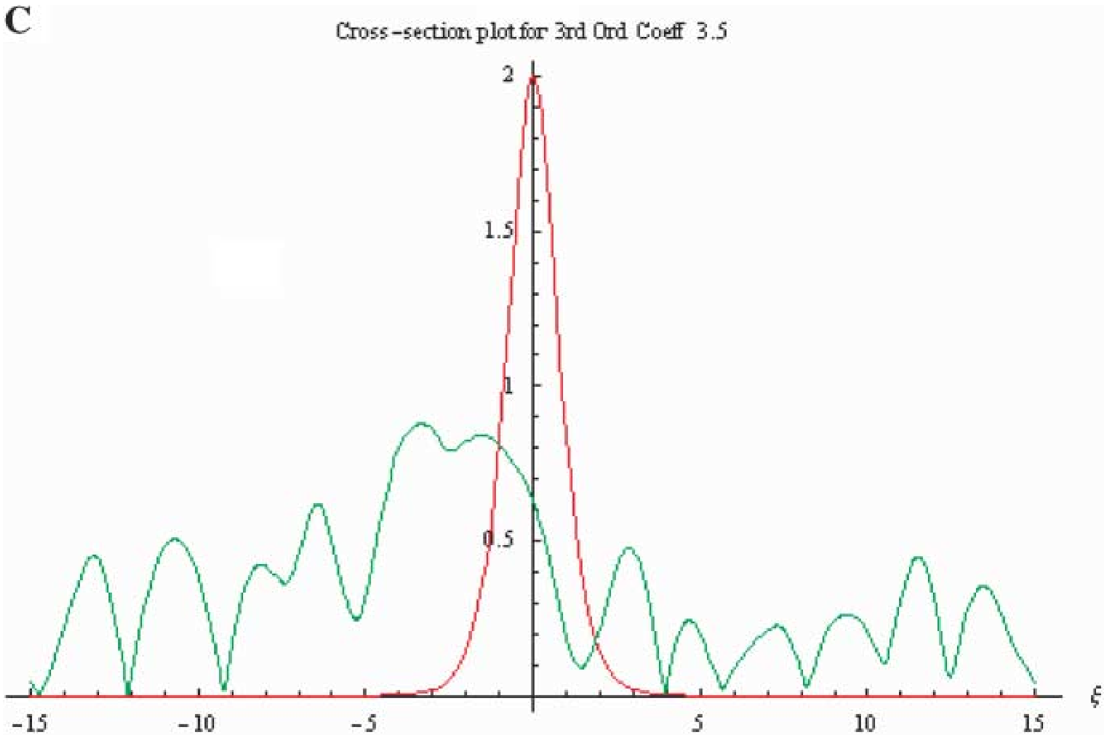

D

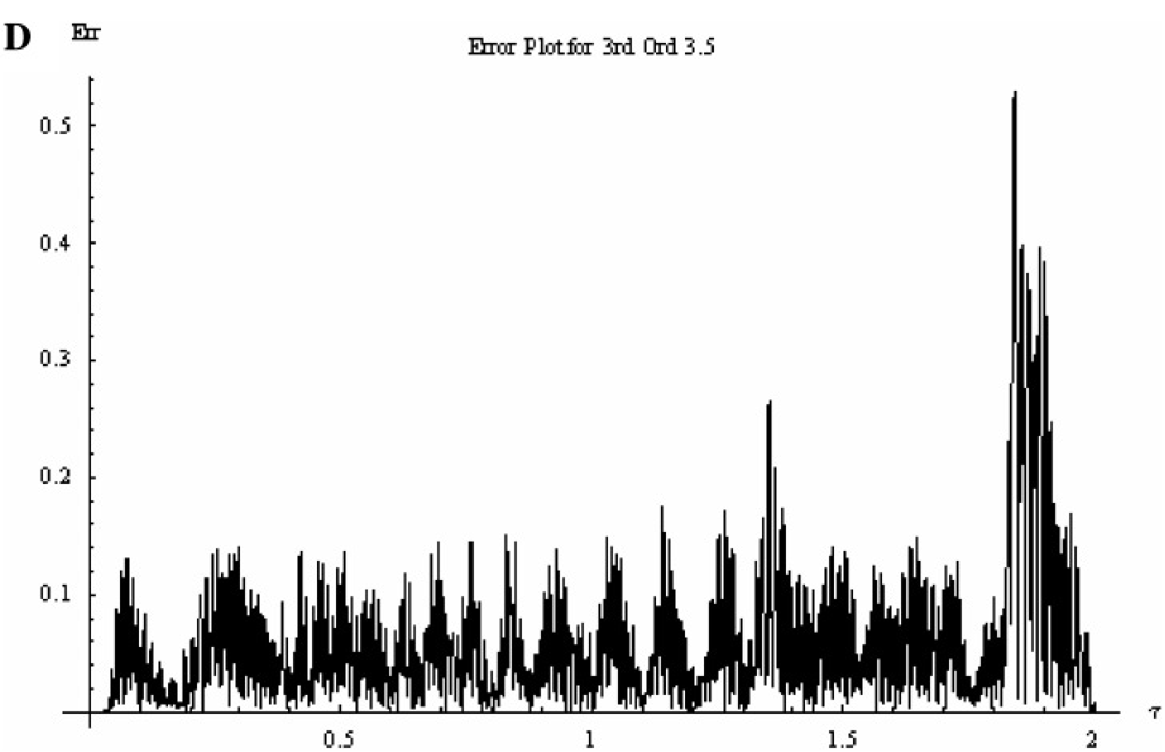

Fig. 5 (continued). (**C**) Here we show the cross-section plot for Figure 5A. (**D**) Here we represent the error plot for Figure 5A.

https://doi.org/10.1017/S0263034605050676 Published online by Cambridge University Press

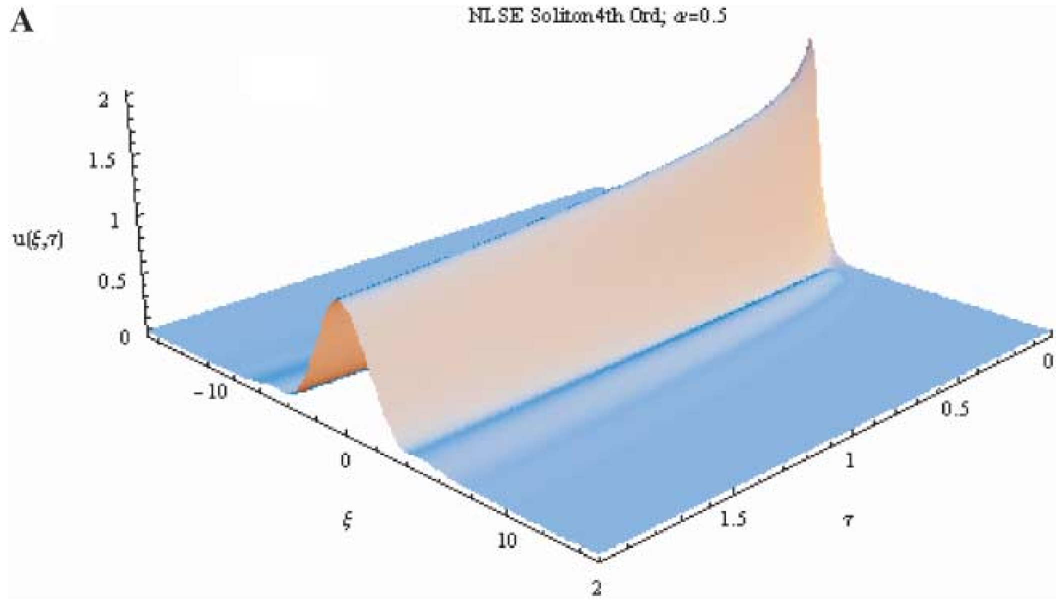

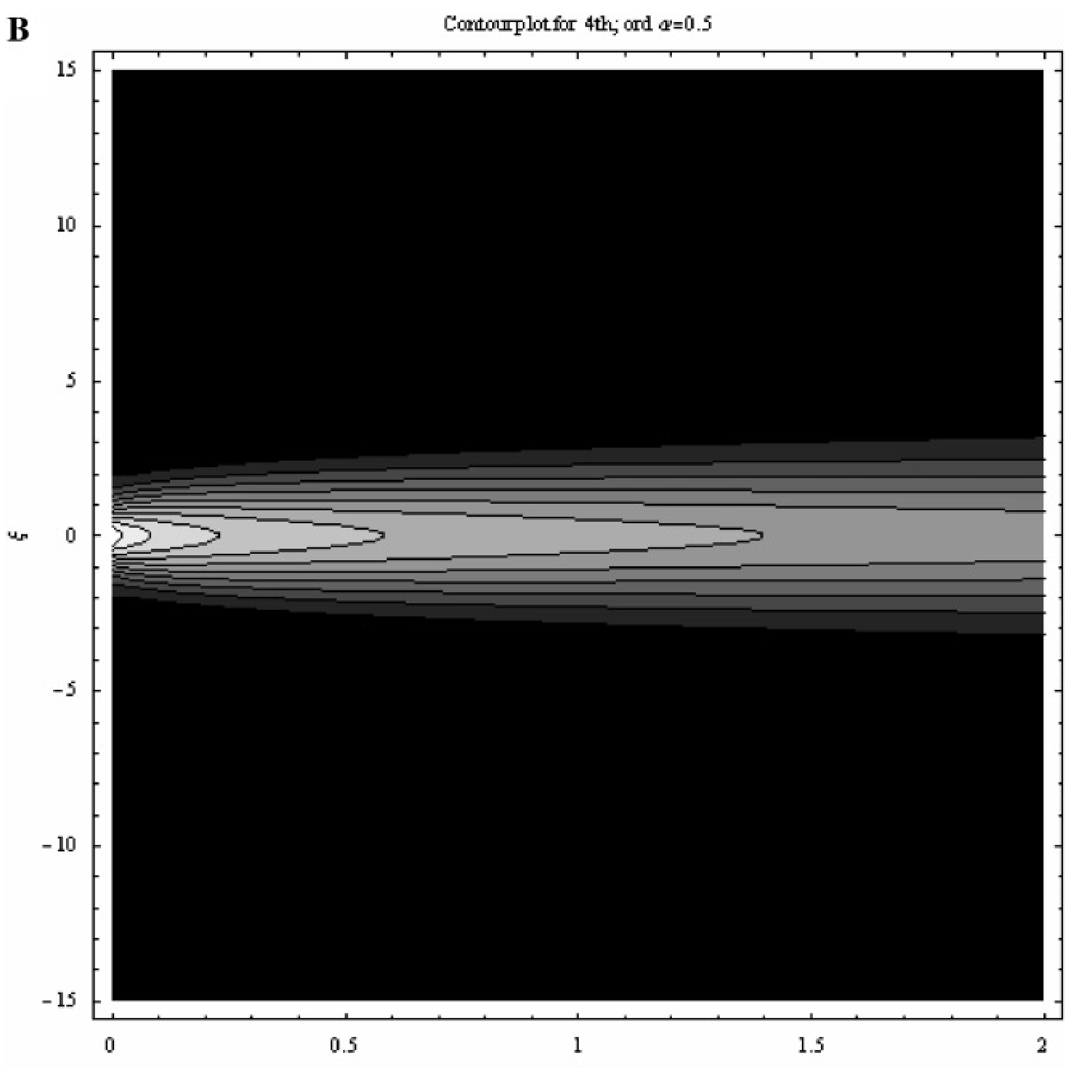

Fig. 6. (**A**) The fourth order at coefficient 0.5. Here we note the characteristic absence of radiation for the square, or even-numbered order, other than that mentioned above with respect to all waves. (**B**) The contour plot for Figure 6A.

https://doi.org/10.1017/S0263034605050676 Published online by Cambridge University Press

C

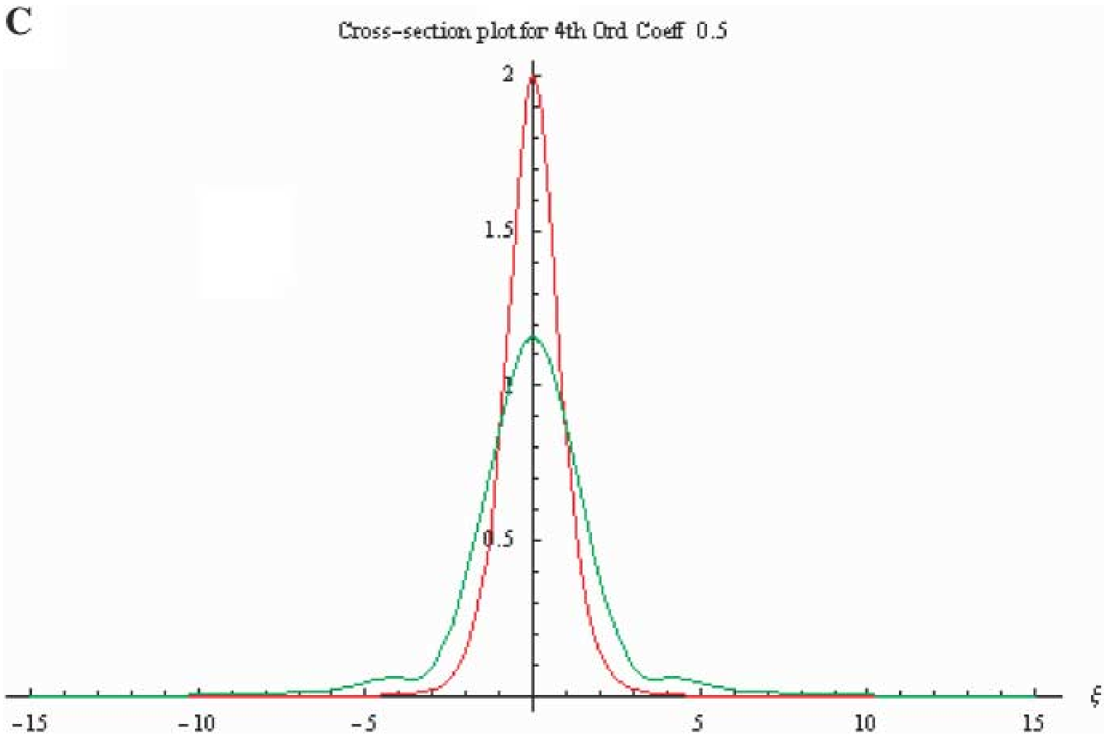

D

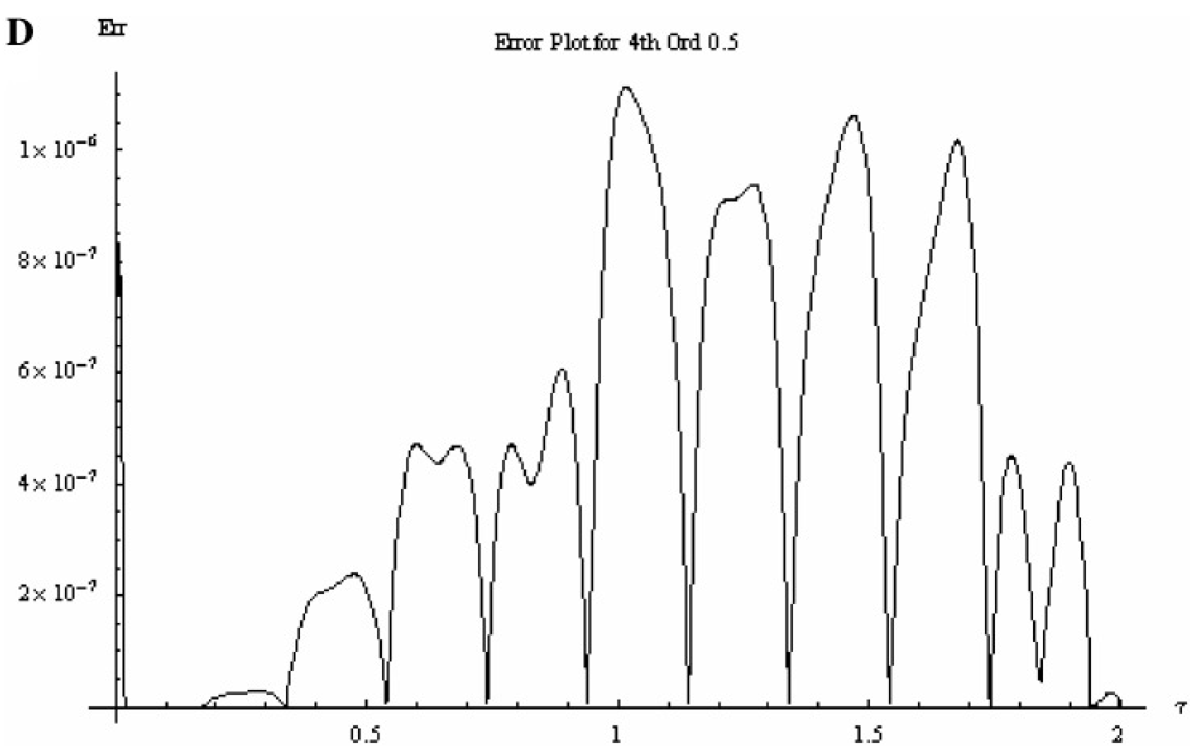

Fig. 6 (continued). (**C**) The cross-sectional plot for Figure 6A. (**D**) The error plot for Figure 6A.

https://doi.org/10.1017/S0263034605050676 Published online by Cambridge University Press

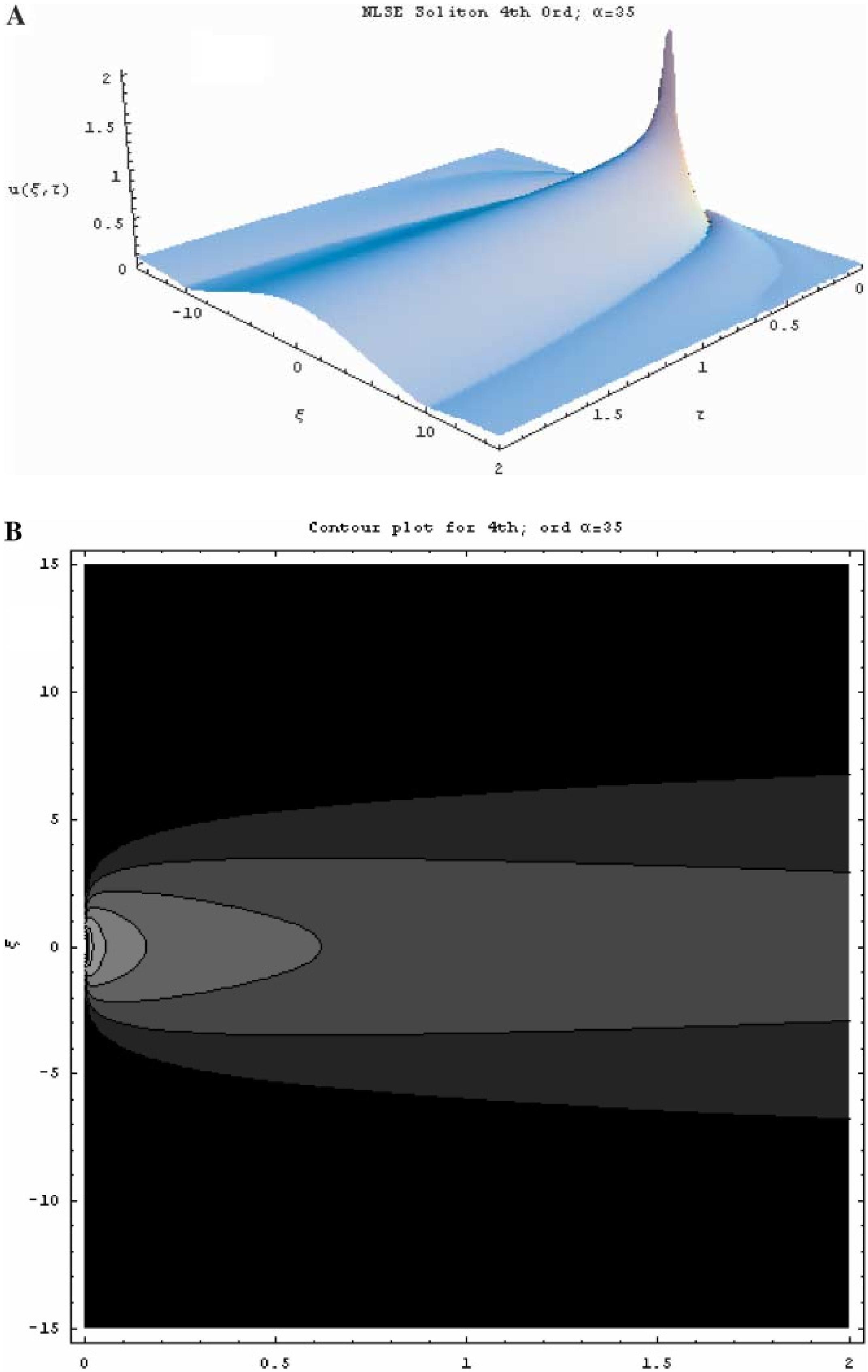

Fig. 7. (**A**) This shows the wave from coefficient of dispersion $\alpha = 35$. Note here the sharp forward peak of the wave, characteristic of self-focusing, but still the absence of radiations. (**B**) Here we show the contour plot for Figure 7A.

https://doi.org/10.1017/S0263034605050676 Published online by Cambridge University Press

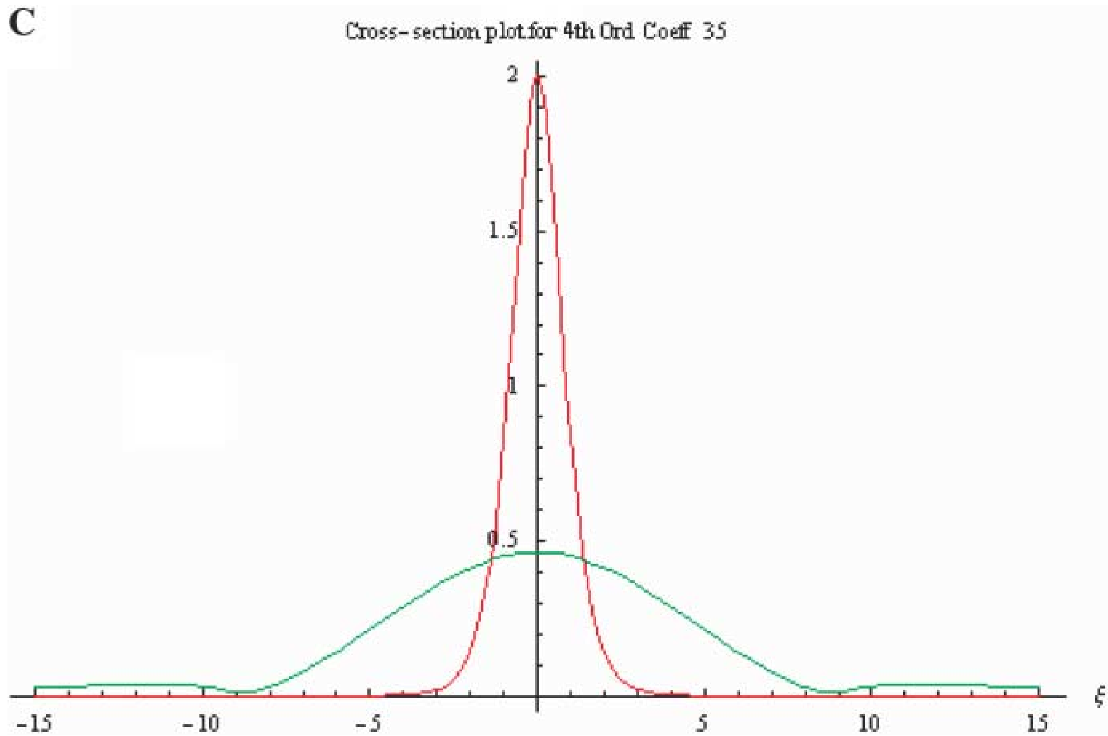

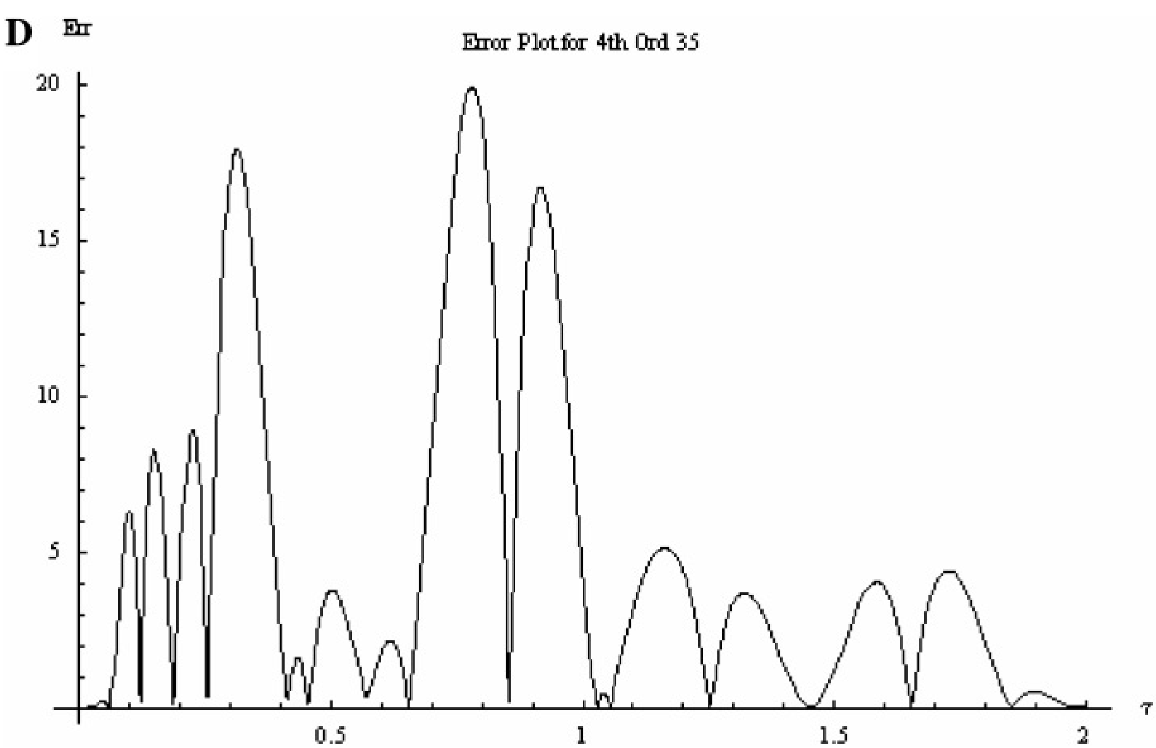

Fig. 7 (continued). (**C**) This is the cross-section plot for Figure 7A. (**D**) Here we show the error plot for Figure 7A.

https://doi.org/10.1017/S0263034605050676 Published online by Cambridge University Press

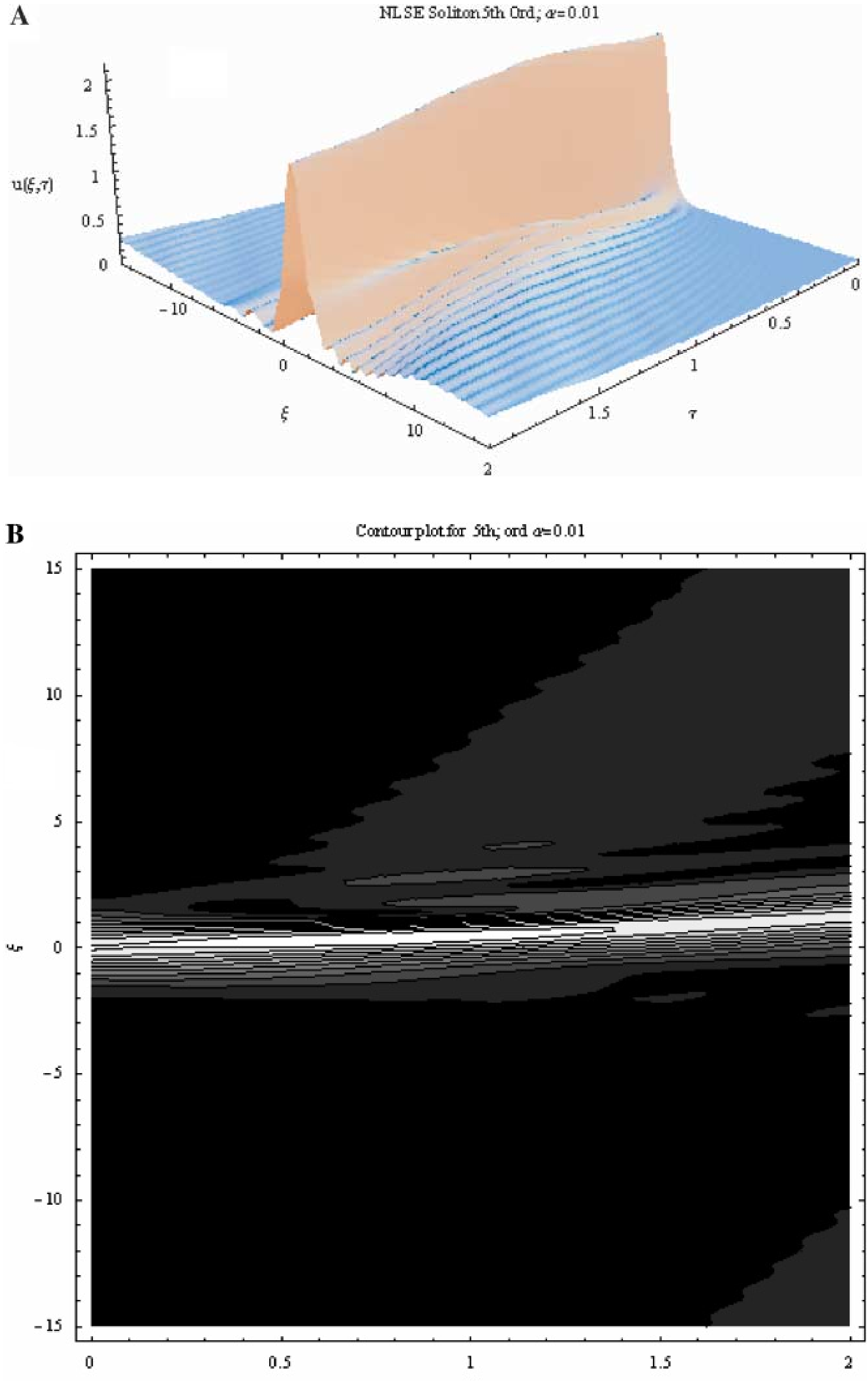

Fig. 8. (**A**) Here we show the graph at the lower end of the fifth order scale. It is easily evident that radiations have begun to show. (**B**) This is the contour plot for Figure 8A.

C

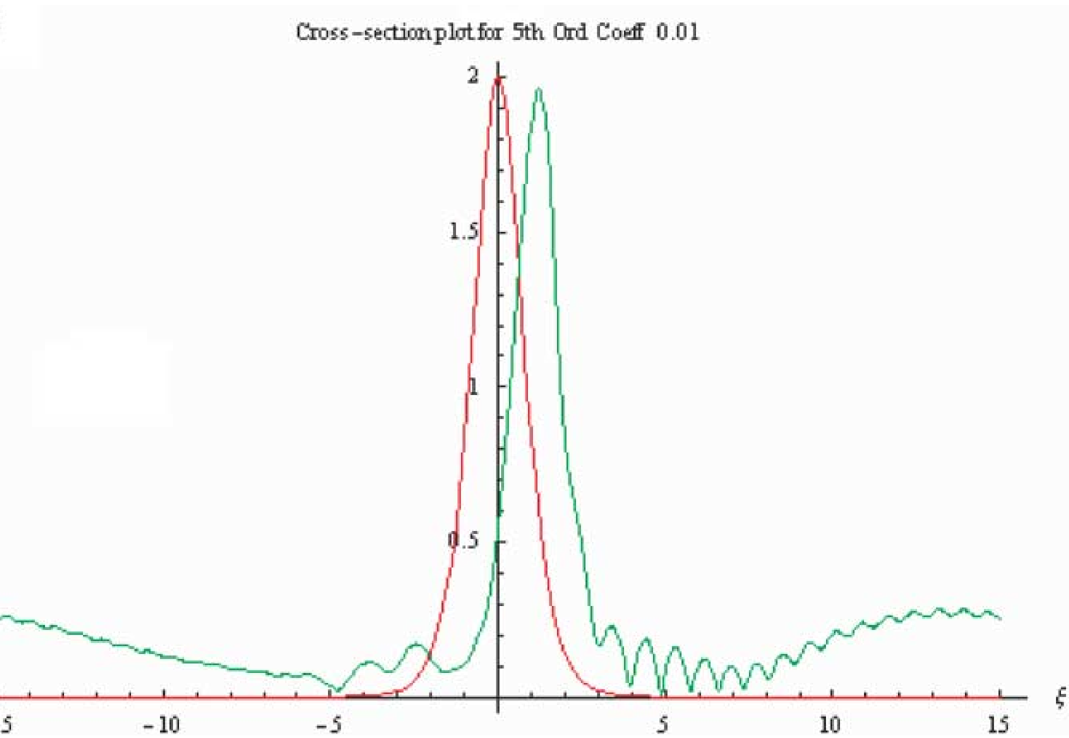

D

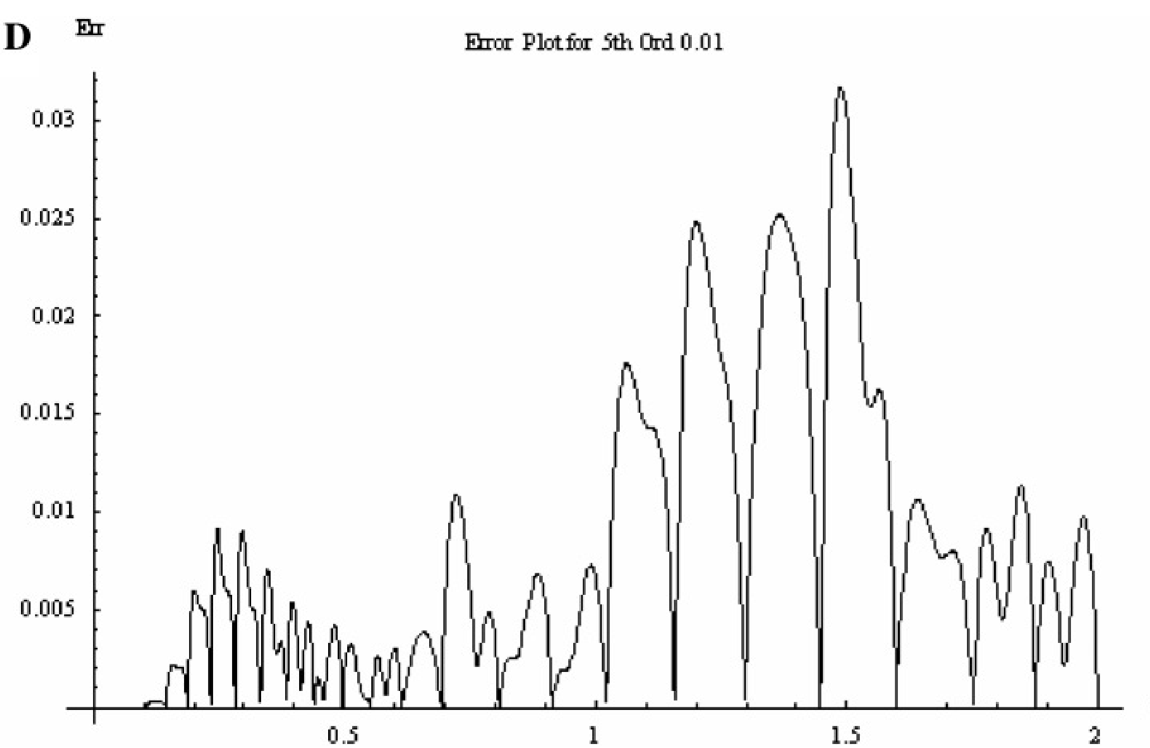

Fig. 8 (continued). (**C**) This is the cross-section plot for Figure 8A. (**D**) The error plot for Figure 8A.

https://doi.org/10.1017/S0263034605050676 Published online by Cambridge University Press

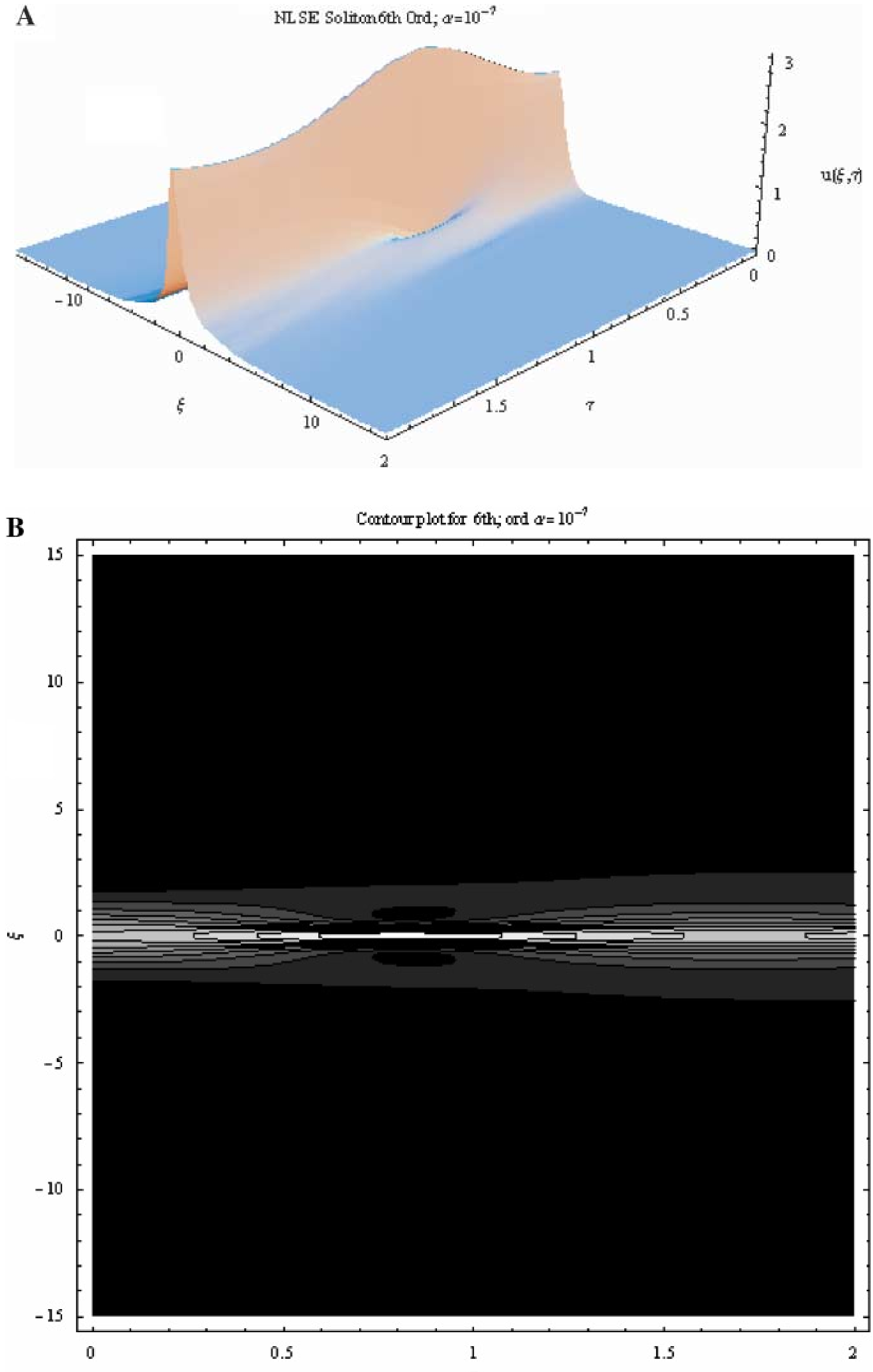

Fig. 9. (**A**) This shows the sixth order soliton at coefficient of dispersion $\alpha = 10^{-7}$. (**B**) This is the contour plot for Figure 9A.

https://doi.org/10.1017/S0263034605050676 Published online by Cambridge University Press

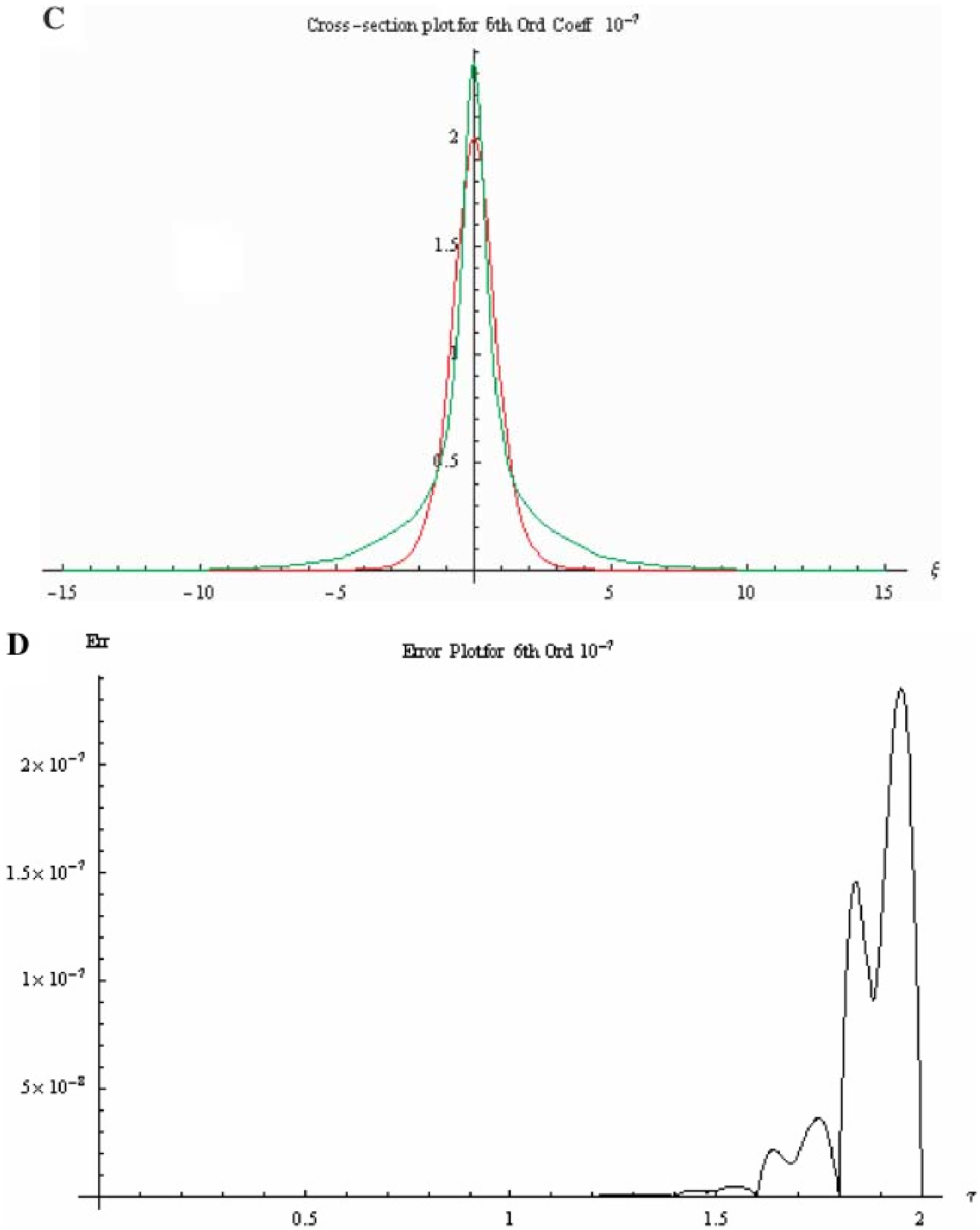

Fig. 9 (continued). (**C**) This shows the cross section plot for Figure 9A. (**D**) Here we show the error plot for Figure 9A.

persion is covered by the work of Karpman (1998) and Karpman and Shagalow (1999). Next we go to Figure 8a. This represents the 3D soliton plot for the fifth order at bottom coefficient 0.01. This is followed by its contour plot in Figure 8b, its cross-section plot in Figure 8c, and its error plot in Figure 8d. After this we go to Figure 9a, where we show the 3D soliton for the sixth order at coefficient 10^{-7}. This is followed by its contour plot in Figure 9b, its cross-section plot in Figure 9c, and its error plot in Figure 9d. Last we show Figure 10a, which represents the highest practical coefficient for the sixth order. We follow this with its contour plot in Figure 10b, its cross-section plot in Figure 10c, and lastly its error plot in Figure 10d.

5. OBSERVATIONS

From the graphic results presented above it has been noted that radiations related to the higher order dispersion factor are only found in cubic orders, that is, where the higher order term in the NLSE is represented by an uneven number. Where the order of magnitude of the dispersion term is quadratic, i.e., it is expressed as an even number, there are

https://doi.org/10.1017/S0263034605050676 Published online by Cambridge University Press

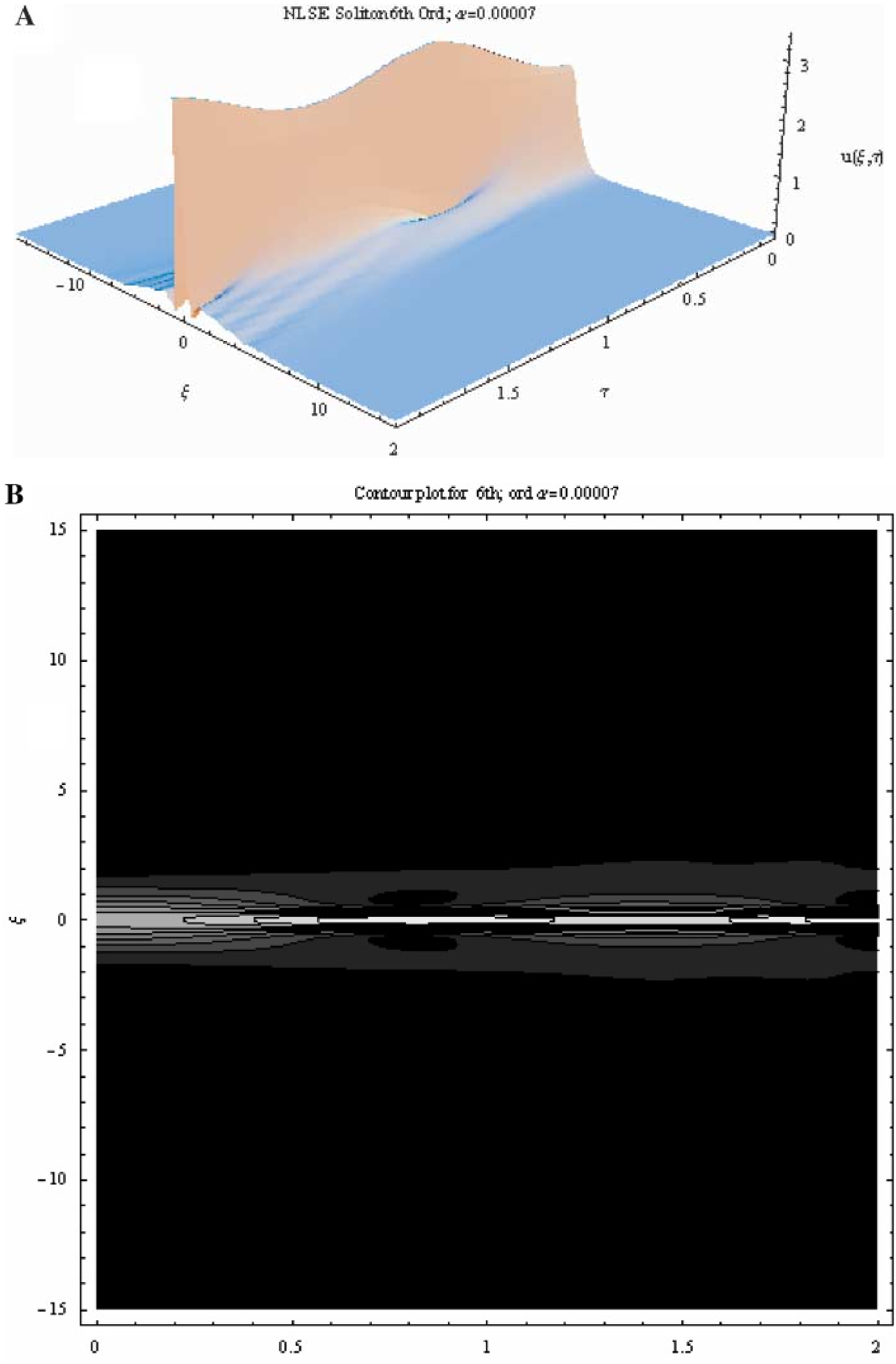

Fig. 10. (**A**) Here we show the soliton produced from a dispersion coefficient of 0.00007. (**B**) The contour plot for Figure 10A.

https://doi.org/10.1017/S0263034605050676 Published online by Cambridge University Press

C

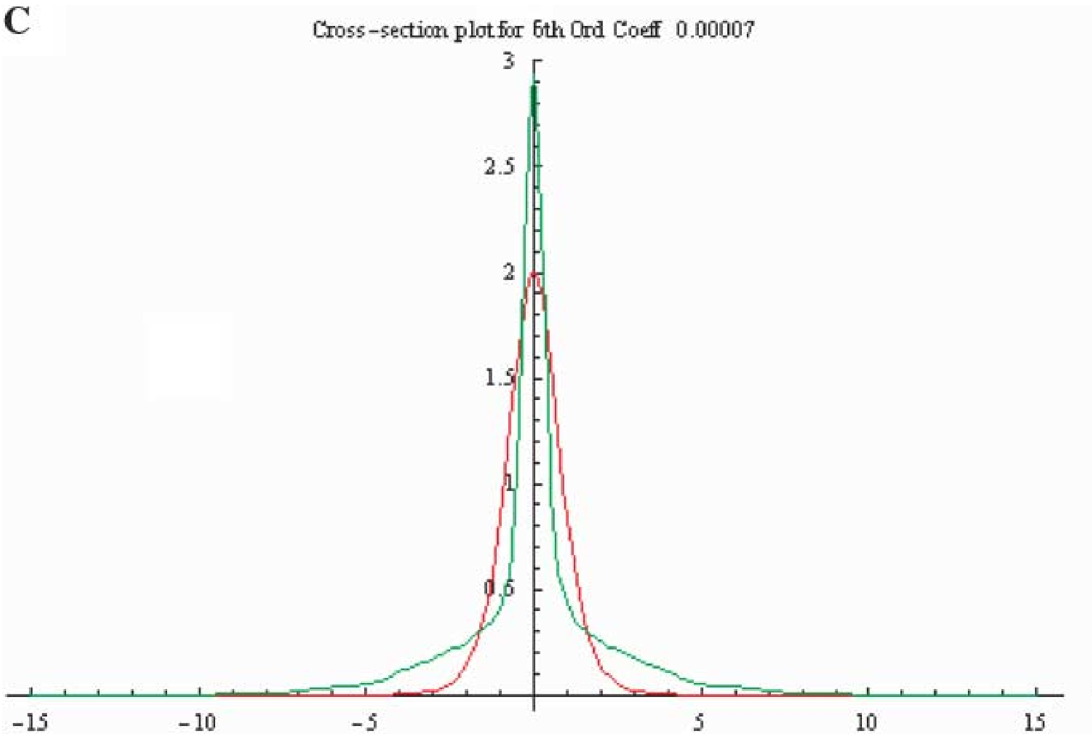

D

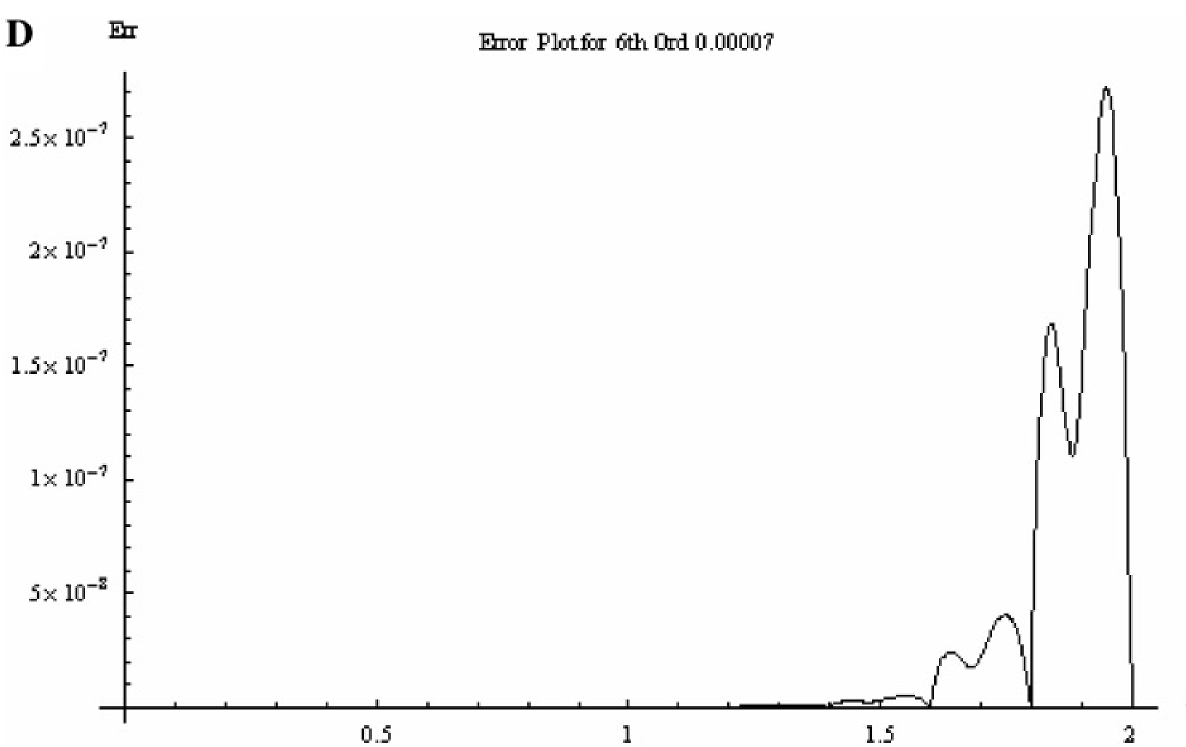

Fig. 10 (continued). (**C**) Shows the cross-section for Figure 10A. (**D**). The error plot for Figure 10A.

https://doi.org/10.1017/S0263034605050676 Published online by Cambridge University Press

no radiations other than the basic waves mentioned above. This leads us to draw far-reaching conclusions.

6. CONCLUSION

The most important conclusion to be drawn in the face of this evidence is that solitonic radiations only occur in the presence of a cubic dispersion term of the NLSE. In the cases where the order of dispersion is quadratic there are no higher order radiations from the soliton. The conclusions to be drawn from this evidence is that, if the solitons can be produced in practice by an input that has no cubic term in its spectrum, then the resulting solitons will be virtually free from radiations. The consequences of this are that if such a soliton were to be employed in the field of fibre optical telecommunications, for instance, there would be virtually none of the factors that cause interference, "crossed lines," etc.

REFERENCES

Akhmediev, N.N. & Ankiewicz, A. (1997). *Solitons, Nonlinear Pulses And Beams*. Canberra: Chapman & Hall.

Beech, R. & Osman, F. (2004). Breaking and Self-Focusing Properties of Korteweg de Vries Solitons. *Proc. IMS2004*, Banff, Canada.

Drazin, G. & Johnson, R.S. (1990). *Solitons: An Introduction*. Cambridge: Cambridge University Press.

Hora, H. (2004). Developments in inertial fusion energy and beam fusion at magnetic confinement. *Laser Part. Beams* **22**, 69–74.

Hora, H. (1991). *Plasmas at High Temperature and Density*. Heidelberg: Springer.

Karpman, V.I. (1998). Evolution of solitons described by higher-order nonlinear Schrödinger equations. *Phy. Lett. A* **244**, 397–400.

Karpman, V.I. & Shagalow, A.G. (1999). Evolution of solitons described by higher-order nonlinear Schrödinger equation. II. Numerical investigation. *Phys. Lett. A* **254**, 319–324.

Osman, F., Castillo, R. & Hora, H. (2000). Focusing and Defocusing of the Nonlinear Paraxial Equation at Laser Plasma Interaction. *Laser Part. Beams* **18**, 73.

Osman, F., Cang, Yu., Hora, H., Evans, P., Cao, L.H., Liu, H., He, X.T., Badziak, J., Parys, A.B., Wolowski, J., Woryna, E., Jungwirth, K., Kraliova, B., Kraska, J., Laska, L., Pfeifer, M., Rohlena, K., Skala, J. & Ullschmied, J. (2004*a*). Two-Fluid Computations to Skin Layer Acceleration. *Laser Part. Beams* **22**, 83–88.

Osman, F., Beech, R. & Hora, H. (2004*b*). Solutions of the nonlinear paraxial equation due to laser-plasma interactions. *Laser Part. Beams* **22**, 69–74.

Wolfram, S. (2003). *The Mathematica Book*. Champaign, IL: Wolfram Media.

Zakharov, V.E. & Shabat, A.B. (1972). Exact theory of two-dimensional self-focusing and one-dimensional self-modulation of waves in nonlinear media. *Sov. Phys. JETP* **34**, 62.